

## A Simple and Effective Strategy To Increase the Sensitivity of Fluorescence Probes in Living Cells

Saki Izumi,<sup>†</sup> Yasuteru Urano, Kenjiro Hanaoka,<sup>†</sup> Takuya Terai,<sup>†</sup> and Tetsuo Nagano<sup>\*,†</sup>

CREST, Japan Science and Technology Agency, 4-8-1 Honcho, Kawaguchi, Saitama, 332-0012, Japan, and Graduate School of Pharmaceutical Sciences, the University of Tokyo, 7-3-1 Hongo, Bunkyo-ku, Tokyo 113-0033, Japan

Received March 30, 2009; E-mail: tlong@mol.f.u-tokyo.ac.jp

**Abstract:** Noninvasive visualization and investigation of interactions among proteins, biomolecules, and enzymes in living cells is an important goal for biologists, and fluorescence probes are powerful tools for this purpose. Because many target molecules are present in only trace amounts, high sensitivity is very important, and it is common to improve the sensitivity of fluorescence probes by focusing on high reaction velocity,  $K_d$ . (Gee, K. R.; Archer, E. A.; Lapham, L. A.; Leonard, M. E.; Zhou, Z.; Bingham, J.; Diwu, Z. *Bioorg. Med. Chem. Lett.* **2000**, *10*, 1515–1518.) So far, we have designed and synthesized various highly sensitive fluorescence probes based on the above concepts. (Gabe, Y.; Urano, Y.; Kikuchi, K.; Kojima, H.; Nagano, T. *J. Am. Chem. Soc.* **2004**, *126*, 3357–3367. Komatsu, K.; Urano, Y.; Kojima, H.; Nagano, T. *J. Am. Chem. Soc.* **2007**, *129*, 13447–13454.) Nevertheless, they were sometimes insufficiently sensitive to detect biomolecules in living cells, despite high chemical sensitivity in cuvette. In this report, we suggest a new approach to increase the sensitivity of fluorescence probes, focusing on their intracellular retention. Since calcein is well-retained, we investigated its structural, chemical, and optical characteristics and found that the iminodiacetic acid group (IAG) is a key structure for the intracellular retention. We next designed and synthesized novel fluorescence probes containing IAGs. They showed superior intracellular retention, making it possible to visualize low concentrations of target molecules that would be difficult to observe with conventional probes and permitting long-term observation in living cells. Improvement of intracellular retention of fluorescence probes holds great promise as a strategy for developing a wide range of highly sensitive probes for studies on various biological phenomena.

### Introduction

Molecular imaging is one of the most effective techniques for noninvasive, quantitative, real-time biological studies of the interactions of biological molecules in living cells. Fluorescence probes are among the most powerful tools for this purpose because of their ease of use, high sensitivity, and high selectivity. The two important requirements for effective fluorescence probes are (1) to react only with the target biomolecule and (2) to show dynamic changes of fluorescence properties, such as fluorescence quantum yield or fluorescence wavelength, upon reaction with the target molecule.

Focusing on the above two points, many fluorescence probes have been developed. To obtain high sensitivity, it is usual to focus on enhancing the affinity of the probes for the target molecule and controlling the fluorescence properties via fluorescence resonance energy transfer (FRET),<sup>2</sup> photoinduced electron transfer (PeT),<sup>3</sup> or intramolecular charge transfer (ICT).<sup>4</sup> We have utilized the PeT mechanism on a fluorescent scaffold to control the fluorescence quantum yield of fluorescein derivatives<sup>5</sup> and developed a variety of fluorescence sensor probes

based on fluorescein.<sup>6–8</sup> This approach has also been applied to rhodamine,<sup>9</sup> boron–dipyrromethene (BODIPY),<sup>1</sup> cyanine,<sup>10</sup> and other scaffolds.

From a chemical, biological viewpoint, fluorescein is one of the most attractive fluorescent dyes because of its high fluorescence quantum yield, solubility in aqueous media, visible light excitation, ease of modification, and ready diffusion in cytosol.<sup>11</sup> It has empirically become clear that fluorescence probes must diffuse in cytosol for the detection of certain kinds of target molecules. Therefore, many fluorescein-based fluorescence probes have been developed, such as Newport Green<sup>12</sup> and Fluo-3,<sup>13,14</sup> which are fluorescent indicators for cytosolic chelatable  $Zn^{2+}$  or  $Ca^{2+}$ . Furthermore, fluorescein is extensively

- (2) Lakowicz, J. R. *Principles of Fluorescence Spectroscopy*, Second Edition, 2nd ed.; Kluwer Academic/Plenum Publisher: New York, 1999.
- (3) De Silva, A. P.; Fox, D. B.; Moody, T. S.; Weir, S. W. *Trans. Biotechnol.* **2001**, *19*, 29–34.
- (4) Grabowski, Z. R.; Rotkiewicz, K.; Rettig, W. *Chem. Rev.* **2003**, *103*, 3899–4031.
- (5) Miura, T.; Urano, Y.; Tanaka, K.; Nagano, T.; Ohkubo, K.; Fukuzumi, S. *J. Am. Chem. Soc.* **2003**, *125*, 8666–8671.
- (6) Kojima, H.; Nakatsubo, N.; Kikuchi, K.; Kawahara, S.; Kirino, Y.; Nagoshi, H.; Hirata, Y.; Nagano, T. *Anal. Chem.* **1998**, *70*, 2446–2453.
- (7) Hirano, T.; Kikuchi, K.; Urano, Y.; Higuchi, T.; Nagano, T. *J. Am. Chem. Soc.* **2000**, *122*, 12399–12400.
- (8) Tanaka, K.; Miura, T.; Umezawa, N.; Urano, Y.; Kikuchi, K.; Higuchi, T.; Nagano, T. *J. Am. Chem. Soc.* **2001**, *123*, 2530–2536.

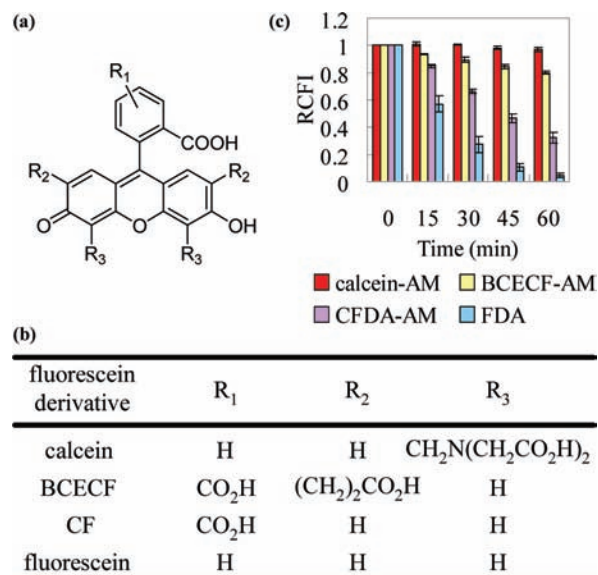
<sup>†</sup>CREST.

(1) Gabe, Y.; Urano, Y.; Kikuchi, K.; Kojima, H.; Nagano, T. *J. Am. Chem. Soc.* **2004**, *126*, 3357–3367.

used not only as a core fluorophore of probes to detect a variety of target biomolecules, especially in cytosol, but also as a fluorescent tag for proteins, DNAs, and other biologically important molecules.<sup>11,15–17</sup> Despite the significant contribution of fluorescein to biological studies, it has been pointed out that its intracellular retention is inadequate, even though it has two negative charges at neutral pH,<sup>18,19</sup> and continuous and prolonged observation is not possible. In short, the concentration of fluorescein-based fluorescence probes and their fluorescent products after reaction with biomolecules cannot be maintained for long at a sufficiently high level for fluorescence detection in living cells, and this impairs the practically achievable sensitivity. We hypothesized that controlling the leakage of fluorescence probes from living cells would be an effective strategy to increase probe sensitivity in living cells. Here we describe an examination of the structural requirements for intracellular retention of a fluorophore. On the basis of the results, we designed and synthesized novel fluorescence probes, and confirmed that they could be used to monitor trace levels of biomolecules that were inaccessible to conventional probes in living cells.

## Results and Discussion

We first attempted to identify an effective structure to improve the intracellular retention of fluorescent dyes. 5-(or 6)-Carboxyfluorescein (CF) has been reported to be well-retained inside living cells,<sup>20,21</sup> and this characteristic is believed to be derived from its carboxyl groups (Figure 1a,b), because hydrophilic molecules should not permeate readily through the lipophilic cell membrane. To investigate how much positive or negative charge is needed to achieve retention of dyes inside cells, we examined the intracellular retention of several well-known fluorescent molecules such as calcein,<sup>22</sup> 2',7'-bis(2-carboxyethyl)-5-(or 6)-carboxyfluorescein (BCECF),<sup>23</sup> CF, and fluorescein (Figure 1a,b). For this purpose, we used acetyl or acetoxymethyl (AM) ester derivatives, calcein-AM, BCECF-AM, CFDA-AM, and fluorescein diacetate (FDA), which are

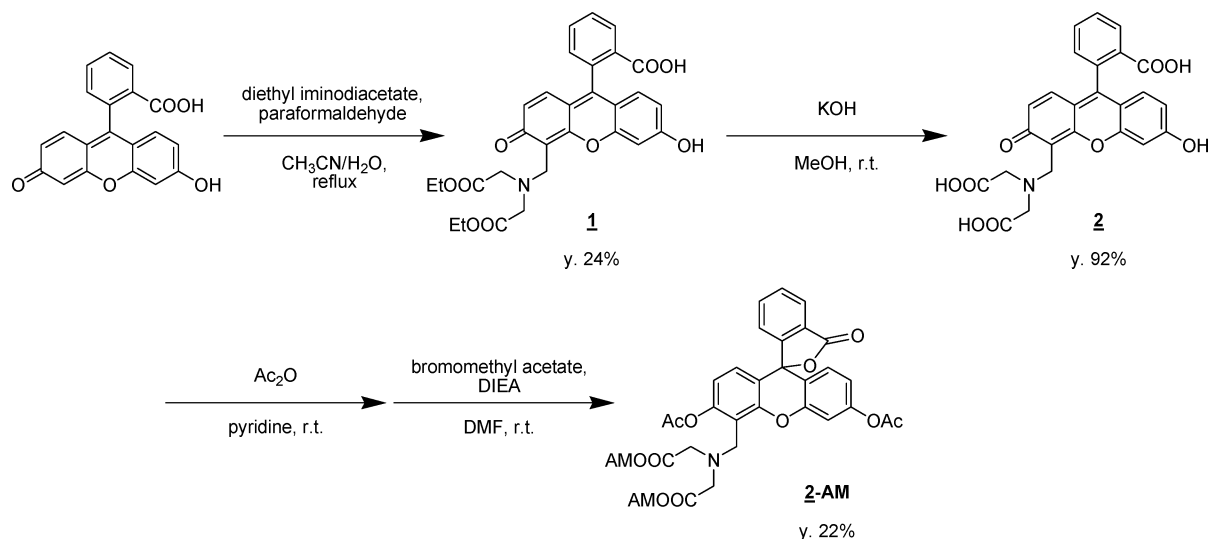


**Figure 1.** (a,b) Structures of fluorescein derivatives. (c) Relative cellular fluorescence intensity (RCFI) of dyes. HL-60 cells were loaded with 1  $\mu$ M cell-permeable acetoxymethyl ester (AM) or diacetate (DA) derivatives of calcein, BCECF, carboxyfluorescein (CF), and fluorescein (F) for 30 min. Then, the dyes were washed out twice, and the course of subsequent changes of fluorescence intensity was measured with flow cytometry (FCM) for 60 min at 37 °C.

membrane-permeable fluorogenic esterase substrates that are hydrolyzed by intracellular esterases to green-fluorescent products. The results indicated that increment of hydrophilicity of the base molecule could improve the intracellular retention, though intracellular retention of BCECF and CF was far from satisfactory (Figure 1c). On the other hand, calcein showed excellent retention. Calcein is a polyanionic fluorescein derivative that has six negative and two positive charges at pH 7.4.<sup>24</sup> However, we thought that its excellent intracellular retention might be due not only to the magnitude of positive or negative charges, but also to features of the structure itself.<sup>25</sup> In biological studies, calcein is commonly used as a dye for live/dead staining,<sup>26</sup> visualizing the vesicle fusion,<sup>27</sup> bone imaging,<sup>28</sup> and so on. It is well-known that various metal ions bind to calcein, and heavy metal ions quench the fluorescence of calcein when they bind to it.<sup>11,29</sup> However, the concentrations of free heavy metal ions are so low in living cells that quenching effects can be ignored in practice, and it has been reported that the fluorescence properties of calcein are little affected by chelation of alkali metal ions or alkaline earth metal ions, which exist at high concentrations in biological systems. However, its chemical properties have never been fully examined<sup>30</sup> and calcein has never been applied as a core fluorophore for the fluorescence sensor probes. Here we investigated the chemical characteristics of calcein's structure in order to exploit its potential for fluorescence sensor probes. The results were applied to the

- (9) Koide, Y.; Urano, Y.; Kikuchi, K.; Kennoku, S.; Kojima, H.; Nagano, T. *J. Am. Chem. Soc.* **2007**, *129*, 10324–10325.
- (10) Sasaki, E.; Kojima, H.; Nishimatsu, H.; Urano, Y.; Kikuchi, K.; Hirata, Y.; Nagano, T. *J. Am. Chem. Soc.* **2005**, *127*, 3684–3685.
- (11) Haugland, R. P. *The Handbook: A Guide to Fluorescent Probes and Labeling Technologies*, 10th ed.; Spence, M. T. Z., Ed.; Molecular Probes, Inc.: Engle, OR, 2005.
- (12) Lukowiak, B.; Vandewalle, B.; Riachy, R.; Kerr-Conte, J.; Gmyr, V.; Belaich, S.; Lefebvre, J.; Pattou, F. *J. Histochem. Cytochem.* **2001**, *49*, 519–527.
- (13) Minta, A.; Kao, J. P. Y.; Tsien, R. Y. *J. Biol. Chem.* **1989**, *264*, 8171–8178.
- (14) Pickering, M.; Pickering, B. W.; Murphy, K. J.; O'Connor, J. J. *J. Neurosci. Methods* **2008**, *173*, 27–33.
- (15) Keppler, A.; Pick, H.; Arrivoli, C.; Vogel, H.; Johnsson, K. *Proc. Natl. Acad. Sci. U.S.A.* **2004**, *101*, 9955–9959.
- (16) Bannwarth, M.; Corrêa, I. R., Jr.; Sztretye, M.; Pouvreau, S.; Fellay, C.; Aebischer, A.; Royer, L.; Johnsson, K. *ACS Chem. Biol.* **2009**, *4*, 179–190.
- (17) Tomat, E.; Nolan, E. M.; Jaworski, J.; Lippard, S. J. *J. Am. Chem. Soc.* **2008**, *130*, 15776–15777.
- (18) Prosperii, E.; Croce, A. C.; Bottiroli, G.; Supino, R. *Cytometry* **1986**, *7*, 70–75.
- (19) Rotman, B.; Papermaster, B. W. *Proc. Natl. Acad. Sci. U.S.A.* **1966**, *55*, 134–141.
- (20) Thomas, J. A.; Buchsbaum, R. N.; Zimniak, A.; Racker, E. *Biochemistry* **1979**, *18*, 2210–2218.
- (21) De Clerck, L. S.; Bridts, C. H.; Mertens, A. M.; Moens, M. M.; Stevens, W. J. *J. Immunol. Methods* **1994**, *172*, 115–124.
- (22) Diehl, H.; Ellingboe, J. L. *Anal. Chem.* **1956**, *28*, 882–884.
- (23) Rink, T. J.; Tsein, R. Y.; Pozzan, T. *J. Biol. Chem.* **1982**, *257*, 189–196.

- (24) Chiu, V. C. K.; Haynes, D. H. *Biophys. J.* **1977**, *18*, 3–22.
- (25) Holyoak, C. D.; Bracey, D.; Piper, P. W.; Kuchler, K.; Coote, P. J. *J. Bacteriol.* **1999**, *181*, 4644–4652.
- (26) Wang, X. M.; Terasaki, P. I.; Rankin, G. W., Jr.; Chia, D.; Zhong, H. P.; Hardy, S. *Hum. Immunol.* **1993**, *37*, 264–270.
- (27) Kendall, D. A.; MacDonald, R. C. *J. Biol. Chem.* **1982**, *257*, 13892–13895.
- (28) Hapidin, H.; Othman, F.; Soelaiman, I.; Shuid, A. N.; Luke, D. A.; Mohamed, N. *J. Bone Miner. Metab.* **2007**, *25*, 93–98.
- (29) Jun, E. J.; Kim, J. A.; Swamy, K. M. K.; Park, S.; Yoon, J. *Tetrahedron Lett.* **2006**, *47*, 1051–1054.

Scheme 1. Synthetic Scheme for Compounds **2** and **2-AM**

design and synthesis of highly sensitive fluorescence probes that were confirmed to be superior to conventional probes in living cells.

**Investigation of the Structure of Calcein.** Initially, we hypothesized that the superior intracellular retention of calcein was due to its distinctive structure with two imino-diacetic acid groups (IAGs), and we synthesized compound **2**, which has only one IAG, in order to test this hypothesis (Scheme 1). Because **2** lacks membrane permeability, we also synthesized a cell-loading derivative, compound **2-AM** (Scheme 1). We then investigated the effect of the IAGs by using living cells loaded with calcein-AM, **2-AM**, and FDA

(Figure 2). In the case of FDA, the fluorescence images of HeLa cells quickly became unclear because of the rapid leakage of fluorescein (Figure 2a); such leakage reduces the sensitivity of fluorescence probes. On the other hand, **2** and calcein, which have one and two IAGs, respectively, were retained well in living cells (Figure 2a,b). This result indicated that introduction of IAG does enhance intracellular retention of dyes, though the extent of their retention may vary from cell line to cell line. However, it appeared that more than two IAGs were required for efficient intracellular retention. Next, we examined the alterations of fluorescence properties provoked by the introduction of IAGs; these results are summarized in Table 1. When IAGs were introduced into fluorescein, the  $pK_a$  value became lower (Figure S1, Supporting Information), and the quantum yields of fluorescence of calcein, **2**, and fluorescein were 0.79, 0.80, and 0.85 at pH 7.4, respectively (Table 1). In brief, two IAGs allowed fluorescence probes to be retained in living cells without impairment of the fluorescence intensity in the physiological pH range. We also examined the photobleaching of calcein and found that it was almost the same as that of fluorescein (Figure S2, Supporting Information). Furthermore, the electrochemical features were examined using cyclic voltammetry in order to see whether or not the PeT mechanism would be applicable to calcein. We found that the reduction potential of calcein is  $-0.73$  V vs SCE at pH 4 and  $-1.01$  V vs SCE at pH 8 (Table 1). These values are similar to those of fluorescein, suggesting that the fluorescence of calcein can be controlled by the PeT mechanism, as is the case for fluorescein.

**Design and Synthesis of a Highly Sensitive Fluorescence Probe for Highly Reactive Oxygen Species (hROS), APC.** Next, we tried to utilize these findings to develop novel fluorescence probes, anticipating that improvement of intracellular retention would lead to high sensitivity. Initially, we focused on reactive oxygen species (ROS) as a target molecule because they are important biological mediators in a wide range of physiological processes.<sup>32,33</sup> We have reported that aryloxyphenols quench the fluorescence of fluorescein via the PeT mechanism and are *O*-dearylated in the ipso-substitution

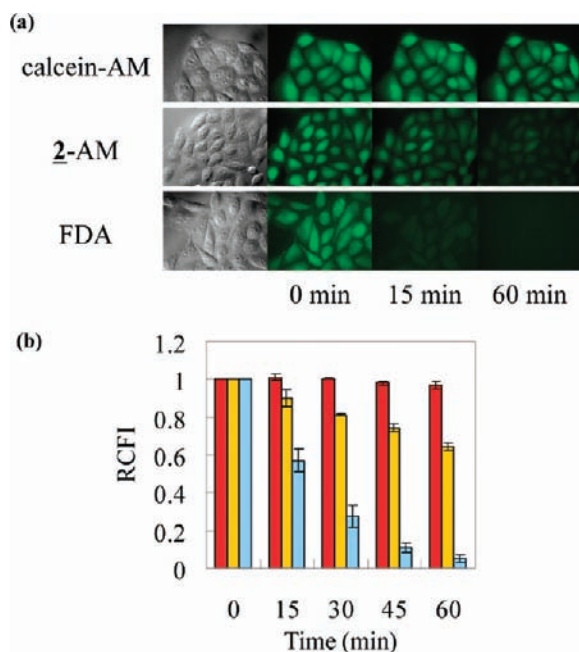


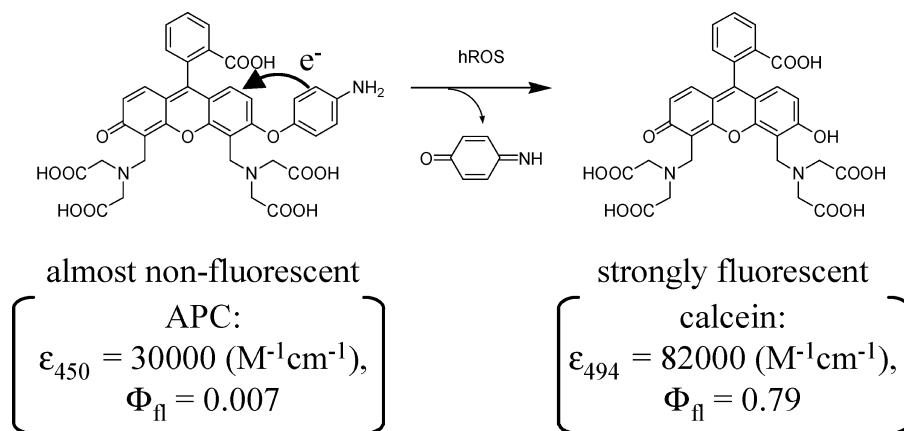
**Figure 2.** (a) Fluorescence images of the change of fluorescence intensity of calcein (100–1100), **2** (100–800), and fluorescein (100–150). (b) RCFI of calcein (red), **2** (orange), and fluorescein (blue). HeLa cells (a) and HL-60 cells (b) were loaded with  $1 \mu\text{M}$  calcein-AM, **2-AM**, and FDA at  $37^\circ\text{C}$  for 30 min. Then, the dyes were washed out twice and the course of subsequent changes of fluorescence intensity was measured by means of microscopy (a) or FCM (b) for 60 min at  $37^\circ\text{C}$ . Exposure time was 100 ms, and ND was 12%.

(30) Wallach, D. F. H.; Steck, T. L. *Anal. Chem.* **1963**, *35*, 1035–1044.  
 (31) Parker, C. A.; Rees, W. T. *Analyst* **1960**, *85*, 587–600.

**Table 1.** Photochemical Properties of Calcein, **2**, and Fluorescein

compound	Abs <sub>max</sub> (nm) <sup>a</sup>	Em <sub>max</sub> (nm) <sup>a</sup>	molar extinction coefficient ( $\times 10^4$ M <sup>-1</sup> cm <sup>-1</sup> ) <sup>a</sup>	fluorescence quantum yield ( $\Phi_f$ ) <sup>b</sup>	reduction potential (V vs SCE) <sup>c</sup>	
					pH 4	pH 8
calcein	494	516	8.2	0.79	-0.73	-1.01
<b>2</b>	492	515	7.3	0.80	-0.73	-1.07
fluorescein	490	515	9.3	0.85	-0.75	-1.04

<sup>a</sup>Data for calcein, **2**, and fluorescein were measured in 0.1 M sodium phosphate buffer, pH 7.4, containing 0.1% DMSO as a cosolvent. <sup>b</sup>For determination of the fluorescence quantum yield, fluorescein in 100 mM aq NaOH (0.85) was used as a fluorescence standard.<sup>31</sup> <sup>c</sup>All data were measured in 0.1 M sodium phosphate buffer (pH 4 and 8), with Ag/Ag<sup>+</sup> as a reference electrode.

**Scheme 2.** Reaction of APC with hROS

manner by highly reactive oxygen species (hROS), such as hydroxyl radical (<sup>•</sup>OH), peroxyxynitrite (ONOO<sup>-</sup>), and hypochlorite (<sup>-</sup>OCl).<sup>34</sup> So, we designed and synthesized a novel fluorescence probe for hROS, aminophenoxycalcein (APC), which was expected to show excellent intracellular retention, because the reaction product of APC with hROS should be calcein (Schemes 2 and 3). Besides APC, we also prepared the acetoxymethyl ester derivative, APC-AM, as a suitable derivative for cell loading.

First, we evaluated the selectivity of APC for various ROS. APC was almost nonfluorescent at every pH examined (Figure S3, Supporting Information) and showed fluorescence increase only upon reaction with <sup>•</sup>OH, ONOO<sup>-</sup>, and <sup>-</sup>OCl (Table 2). HPLC analysis confirmed that this increment of fluorescence was due to formation of calcein (Figure S4, Supporting Information). Furthermore, the fluorescence intensity reached the maximum immediately and increased dose-dependently in response to addition of hROS (Figure S5, Supporting Information). On the other hand, weakly reactive oxygen species caused no change in the fluorescence intensity. Next, we examined APC in an enzymatic system. The HRP/H<sub>2</sub>O<sub>2</sub> system is well-known to generate hROS, and APC could also detect hROS in this system (Figure S6, Supporting Information). These results demonstrated that APC has high selectivity for hROS and further indicate that IAGs can be introduced into xanthene without altering the characteristic properties of fluorescence probes.

Next, we applied APC-AM to HL-60 cells, which are known to produce a large amount of hROS, such as HOCl, when they are stimulated,<sup>9</sup> in order to examine whether or not intracellular retention of APC was enhanced. We loaded APC-AM (1 μM; 0.1% DMF as a cosolvent) or APF (1 μM;

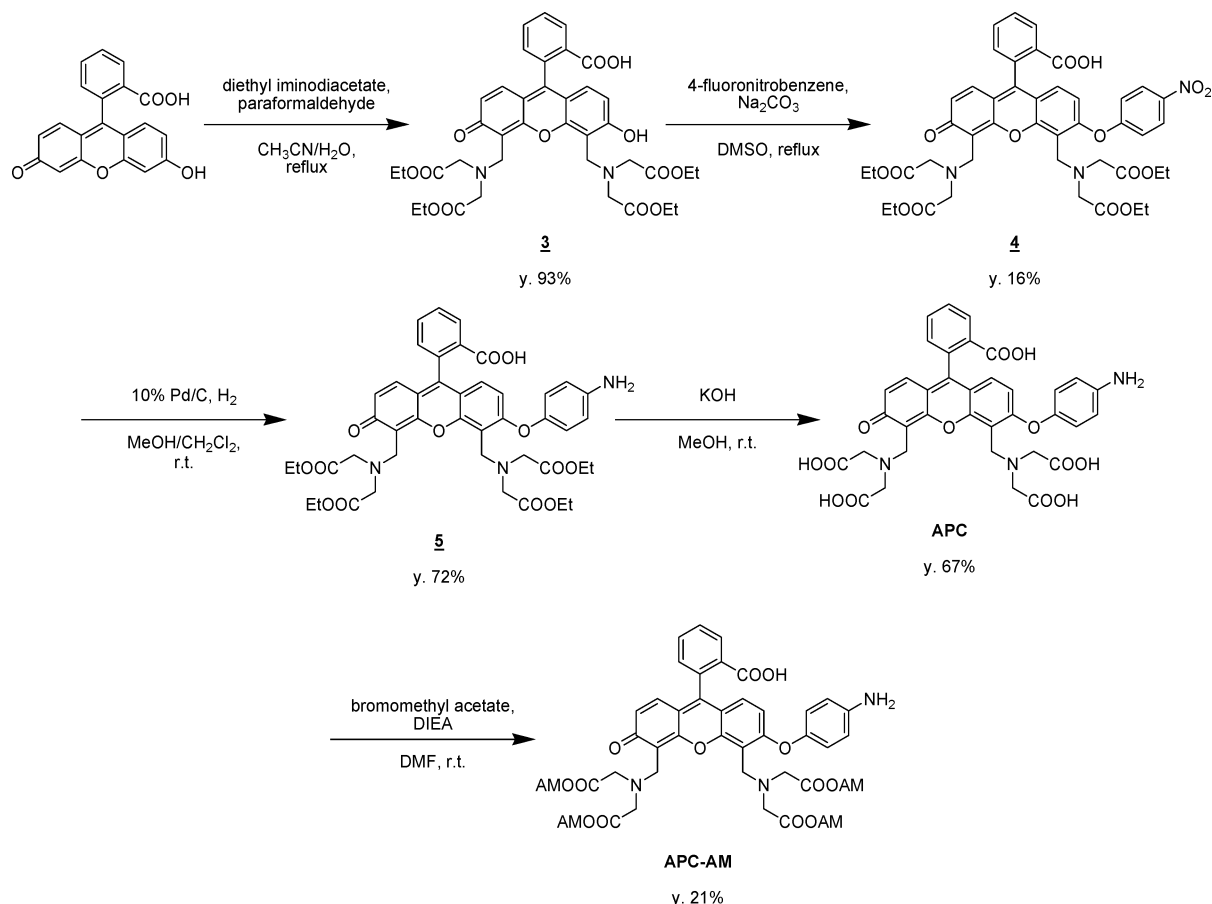
0.02% DMF as a cosolvent) into HL-60 cells for 30 min. APF is a fluorescein-based fluorescence probe for hROS, and we used it as a control.<sup>35</sup> We observed the intensity of intracellular fluorescence after various periods of stimulation with 100 μM H<sub>2</sub>O<sub>2</sub> by means of FCM analysis (Figure 3a). In the case of APF, the fluorescence intensity initially increased upon stimulation and decreased after 10 min. With APC-AM, on the other hand, the fluorescence intensity continued to increase for over 30 min and became much more intense than that of APF.

Moreover, we evaluated the intracellular retention of the reaction product of APC with hROS under physiological conditions, because it is also important that the fluorescence intensity should be stable in long-term experiments, as well as that the fluorescence increase should be large. To confirm the high intracellular retention of APC, we followed the intracellular fluorescence intensity after removal of the stimulus (Figure 3b). HL-60 cells stimulated with 100 μM H<sub>2</sub>O<sub>2</sub> for 10 min were washed to remove H<sub>2</sub>O<sub>2</sub> and their intracellular fluorescence intensity was measured every 15 min with FCM. In the case of APF, the fluorescence intensity decreased as time passed, falling to only 17% of the initial intensity after 60 min. However, in the case of APC-AM, the fluorescence intensity hardly decreased over this period. Further, we applied APC-AM to image hROS inside HL-60 cells by means of fluorescence microscopy. As shown in Figure 3c–f, APC-AM could visualize hROS much more clearly than could APF. These results suggested that introduction of IAGs may largely prevent dye loss from the cells and also support our idea that enhancing intracellular retention is a very effective strategy for improving the sensitivity and reliability of detection of target molecules.

(32) Winterbourn, C. C. *Nat. Chem. Biol.* **2008**, *4*, 278–286.

(33) Wiseman, H.; Halliwell, B. *Biochem. J.* **1996**, *313*, 17–29.

Scheme 3. Synthetic Scheme for APC and APC-AM

Table 2. Fluorescence Increase of APC and APF<sup>a</sup> in Various ROS Generating Systems<sup>34</sup>

ROS	APC	APF
$\cdot\text{OH}^b$	33	70
$\text{ONOO}^-c$	19	28
$^-\text{OCl}^d$	640	528
$^1\text{O}_2^e$	2	2
$\text{O}_2^{-\cdot f}$	<1	<1
$\text{H}_2\text{O}_2^g$	<1	<1
$\text{NO}^h$	<1	4
autoxidation <sup>i</sup>	<1	<1

<sup>a</sup> APC (final 10  $\mu\text{M}$ ; 0.1% DMF as a cosolvent) or APF (final 10  $\mu\text{M}$ ; 0.02% DMF as a cosolvent) was added to sodium phosphate buffer (0.1 M; pH 7.4). The fluorescence intensity of dyes was measured at 516 and 515 nm with excitation at 494 and 490 nm, respectively.

<sup>b</sup> Ferrous perchlorate (final 100  $\mu\text{M}$ ) and  $\text{H}_2\text{O}_2$  (final 1 mM) were added and the fluorescence intensity was immediately measured.

<sup>c</sup>  $\text{ONOO}^-$  (final 3  $\mu\text{M}$ ) was added and the mixture was stirred at 37  $^\circ\text{C}$  for 30 min.

<sup>d</sup>  $\text{NaOCl}$  (final 3  $\mu\text{M}$ ) was added and the mixture was stirred at 37  $^\circ\text{C}$  for 30 min.

<sup>e</sup> 3-(1,4-Dihydro-1,4-epidioxy-1-naphthyl)-propionic acid (EP-1; 100  $\mu\text{M}$ ) was added and the mixture was stirred at 37  $^\circ\text{C}$  for 30 min.

<sup>f</sup> Xanthine oxidase (final 10  $\mu\text{M}$ ) and HPX (final 10  $\mu\text{M}$ ) were added and the mixture was stirred at 37  $^\circ\text{C}$  for 30 min.

<sup>g</sup>  $\text{H}_2\text{O}_2$  (final 100  $\mu\text{M}$ ) was added and the mixture was stirred at 37  $^\circ\text{C}$  for 30 min.

<sup>h</sup> 1-Hydroxy-2-oxo-3-(*N*-methyl-3-aminopropyl)-3-methyl-1-triazene (NOC 7; 10  $\mu\text{M}$ ) was added and the mixture was stirred at 37  $^\circ\text{C}$  for 30 min.

<sup>i</sup> Dye solution was placed under a fluorescent lamp for 2.5 h.

**Design and Synthesis of Highly Sensitive Fluorescence Probe for Nitric Oxide, DCI-DA Cal.** We next employed the same design strategy to develop another novel fluorescence probe, this time for reactive nitrogen species (RNS), to

confirm that improving the retention of fluorescence probes generally leads to enhancement of sensitivity. Nitric oxide (NO) is a significant participant in the physiologic control of vasodilation, renal function, platelet aggregation, and so on.<sup>36</sup> Since NO is also suggested to be important in reperfusion, arteriosclerosis, and cerebral infarction,<sup>37</sup> there is a need to detect NO sensitively in living cells. However, this remains a challenge, because the NO concentration is low and NO is unstable.

We previously developed DAFs as sensitive fluorescence probes for NO;<sup>6</sup> however, their sensitivity is sometimes insufficient to measure NO in living cells. Hence, we designed and synthesized dichlorodiaminocalcein (DCI-DA Cal) from compound **6** as a novel fluorescence probe for NO (Schemes 4 and 5). The reason for using a chlorinated fluorophore is that it is difficult to introduce diethyl iminodiacetic acid groups into a normal xanthene fluorophore. Fluorescence of DCI-DA Cal is well-quenched via the PeT mechanism (Figure

(34) Setsukinai, K.; Urano, Y.; Kikuchi, K.; Higuchi, T.; Nagano, T. *J. Chem. Soc., Perkin Trans. 2* **2000**, 2453–2457.

(35) Setsukinai, K.; Urano, Y.; Kakinuma, K.; Majima, H. J.; Nagano, T. *J. Biol. Chem.* **2003**, 278, 3170–3175.

(36) Leo, R.; Protico, D.; Iuliano, L.; Pulcinelli, F. M.; Ghiselli, A.; Pignatelli, P.; Colavita, A. R.; FitzGerald, G. A.; Violi, F. *Circulation* **1997**, 95, 885–891.

(37) Kakoki, M.; Hirata, Y.; Hayakawa, H.; Suzuki, E.; Nagata, D.; Tojo, A.; Nishimatsu, H.; Nakanishi, N.; Hattori, Y.; Kikuchi, K.; Nagano, T.; Omata, M. *J. Am. Soc. Nephrol.* **2000**, 11, 301–309.

(38) Iyengar, R.; Stuehr, D. J.; Marletta, M. A. *Proc. Natl. Acad. Sci. U.S.A.* **1987**, 84, 6369–6373.

(39) Parbhakar, P.; Thatte, H. S.; Goetz, R. M.; Cho, M. R.; Golan, D. E.; Michel, T. *J. Biol. Chem.* **1998**, 273, 27383–27388.

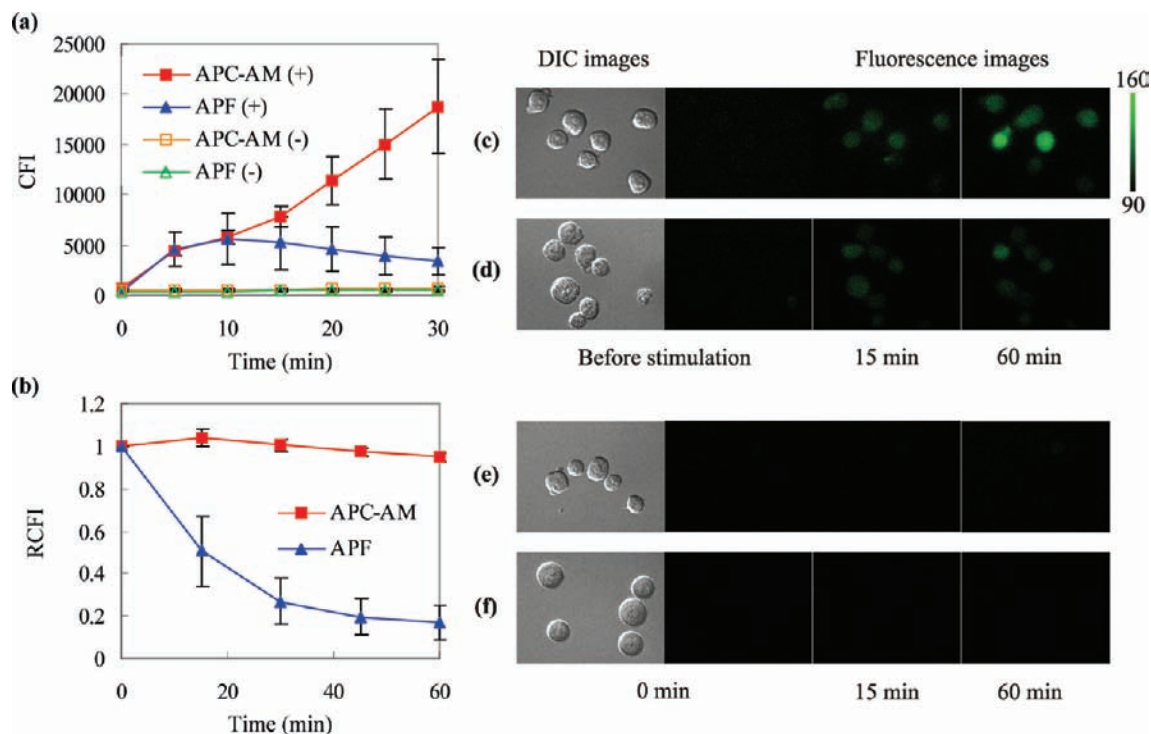
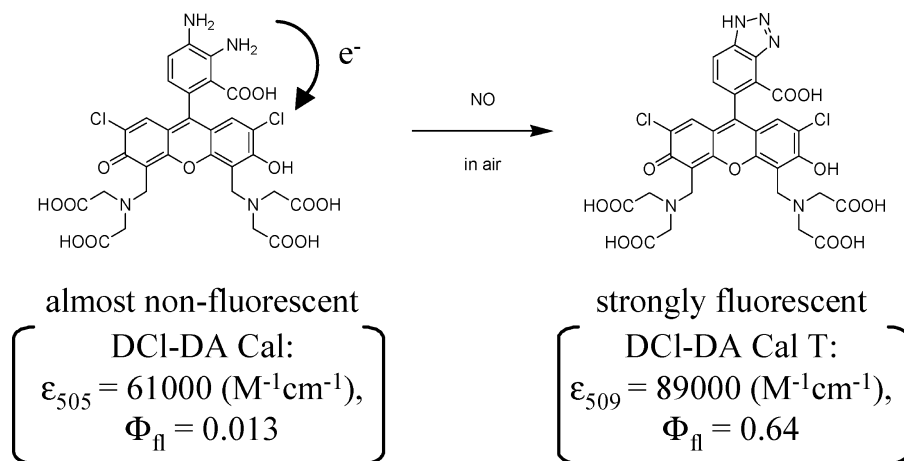


**Figure 3.** Detection of hROS generation with APC or APF. APC-AM (1  $\mu$ M; 0.1% DMF as a cosolvent) or APF (1  $\mu$ M; 0.02% DMF as a cosolvent) was loaded into HL-60 cells for 30 min. APC-AM was then washed out twice, while APF was not: (a) Change of cellular fluorescence intensity (CFI) measured with FCM when HL-60 cells were stimulated with 100  $\mu$ M  $\text{H}_2\text{O}_2$  [APC-AM (+), APF (+)] or not stimulated [APC-AM (-), APF (-)] for various stimulation times (0–30 min). (b) Change of RCFI after 10 min stimulation with 100  $\mu$ M  $\text{H}_2\text{O}_2$ . (c–f) DIC images and fluorescence images of HL-60 cells that had been loaded with APC-AM (c, e) or APF (d, f). Parts c and d were measured before and after stimulation with 100  $\mu$ M  $\text{H}_2\text{O}_2$  for 15 or 60 min and parts e and f were measured after 0, 15, and 60 min without stimulation. Exposure time was 500 ms, and ND was 12%.

**Scheme 4.** Reaction of APC with hROS



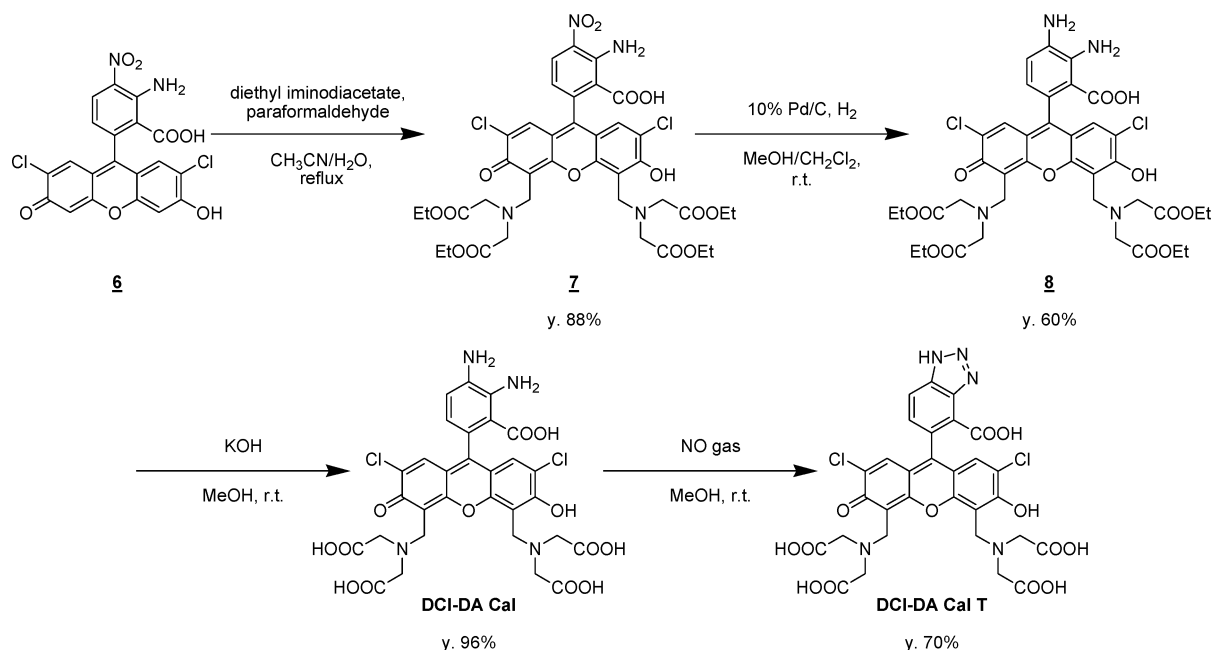
S7, Supporting Information) and the fluorescence quantum yield is 0.013 at pH 7.4. When DCI-DA Cal reacts with NO in air, it is expected that the triazole compound, DCI-DA Cal T, will be produced and will emit strong fluorescence.

First, we examined the reactivity of DCI-DA Cal with various ROS. The results are summarized in Table 3. We also used fluorescein-based fluorescence probes, DAF-2 and DAF-4, as controls.<sup>6</sup> The reactivity experiments revealed a pronounced increase of fluorescence intensity when DCI-DA Cal reacted with NO and  $\text{ONOO}^-$ . Data in Table 3 also show that the values of fluorescence increment of DAF-2 and DAF-4 are similar to that of DCI-DA Cal, and they have almost the same reactivity in cuvette. Further, we confirmed

that the increase of fluorescence intensity of DCI-DA Cal was attributable to the formation of DCI-DA Cal T by purifying and identifying the fluorescent product after the reaction with NO gas (Scheme 5) by means of HPLC (Figure S8, Supporting Information). We also examined the effect of pH on the fluorescence intensity of DCI-DA Cal and DCI-DA Cal T (Figure S7, Supporting Information). DCI-DA Cal was well-quenched at every pH examined, whereas the fluorescence intensity of DCI-DA Cal T was high in the physiological range and its fluorescence quantum yield was 0.64 at pH 7.4.

As a membrane-permeable fluorescence probe, we also prepared DCI-DA Cal-AM, in which the phenolic hydroxyl group and

Scheme 5. Synthetic Scheme for DCI-DA Cal and DCI-DA Cal T

Table 3. Fluorescence Increase of DCI-DA Cal, DAF-2 and DAF-4<sup>a</sup> in Various ROS Generation Systems

ROS	DCI-DA Cal	DAF-2	DAF-4
$\cdot\text{OH}^b$	3	<1	<1
$\text{ONOO}^{-c}$	24	6	9
$\text{OCl}^{-d}$	5	2	5
$^1\text{O}_2^e$	<1	2	<1
$\text{O}_2^{-f}$	<1	<1	<1
$\text{H}_2\text{O}_2^g$	<1	<1	<1
$\text{NO}^h$	70	82	76
autoxidation <sup>i</sup>	<1	<1	<1

<sup>a</sup> DCI-DA Cal, DAF-2, or DAF-4 (final 10  $\mu\text{M}$ ; 0.1% DMF as a cosolvent) was added to sodium phosphate buffer (0.1 M; pH 7.4). The fluorescence intensity of dyes was measured at 531, 515, and 531 nm with excitation at 509, 490, and 505 nm, respectively. <sup>b</sup> Ferrous perchlorate (final 100  $\mu\text{M}$ ) and  $\text{H}_2\text{O}_2$  (final 1 mM) were added, and the fluorescence intensity was immediately measured. <sup>c</sup>  $\text{ONOO}^-$  (final 3  $\mu\text{M}$ ) was added and the mixture was stirred at 37  $^\circ\text{C}$ . <sup>d</sup>  $\text{NaOCl}$  (final 10  $\mu\text{M}$ ) was added and the mixture was stirred at 37  $^\circ\text{C}$  for 30 min. <sup>e</sup> EP-1 (final 100  $\mu\text{M}$ ) were added, and the mixture was stirred at 37  $^\circ\text{C}$  for 30 min. <sup>f</sup> Xanthine oxidase (10  $\mu\text{M}$ ) and HPX (final 10  $\mu\text{M}$ ) was added and the mixture was stirred at 37  $^\circ\text{C}$  for 30 min. <sup>g</sup>  $\text{H}_2\text{O}_2$  (100  $\mu\text{M}$ ) was added and the mixture was stirred at 37  $^\circ\text{C}$  for 30 min. <sup>h</sup>  $\text{NO}$  7 (final 10  $\mu\text{M}$ ) was added and the mixture was stirred at 37  $^\circ\text{C}$  for 30 min. <sup>i</sup> Dye solution was placed under a fluorescent lamp for 2.5 h.

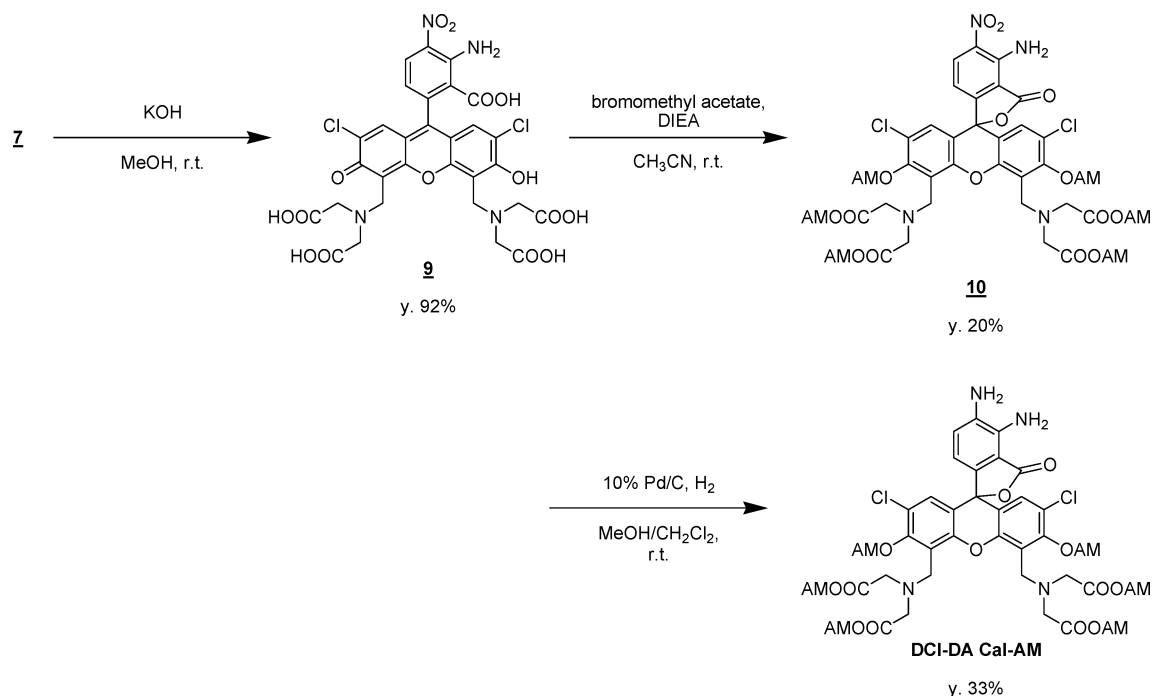
carboxyl group are protected as an acetoxymethyl ester (Scheme 6). It is general to protect phenolic hydroxyl groups with acetyl groups, but this protecting group is easily deprotected at pH 7.4 when a halogen group is present in xanthene because of the low  $\text{pK}_a$  of the phenolic hydroxyl group. There are no reports about the protection of a phenolic hydroxyl group of xanthene with acetoxymethyl ester, so we investigated the stability of this protecting group at pH 7.4 (Figure S9, Supporting Information). The increment of absorption around 505 nm was observed only in the presence of esterase; there was no change of the absorbance spectrum in normal PBS, pH 7.4. These results suggested that the acetoxymethyl ester stably protects the phenolic hydroxyl group under physiological conditions.

Next, to examine how well DCI-DA Cal is retained in living cells, we compared DCI-DA Cal-AM with DAF-2 DA

and DAF-4 DA.<sup>6</sup> We loaded DCI-DA Cal-AM into HeLa cells and examined whether DCI-DA Cal could detect intracellular NO or not. All of the dyes, as shown in Figure 4a–f, could detect NO generated from 1-hydroxy-2-oxo-3-(*N*-methyl-3-aminopropyl)-3-methyl-1-triazene (NOC 7), but the fluorescence intensity of the background also increased when DAF-2 DA and DAF-4 DA were used. This rise of background fluorescence should be derived from leakage of the triazole compounds, DAF-2 T and DAF-4 T,<sup>6</sup> produced in HeLa cells and also from the reaction of NO and fluorescence probes that leaked from the cells. To examine the leakage of triazole compounds DCI-DA Cal T, DAF-2 T, and DAF-4 T, the following experiment was done (Figure 4g–i). After addition of NOC 7 for 10 min to HeLa cells preloaded with DCI-DA Cal-AM, DAF-2 DA, or DAF-4 DA, the cells were washed twice, and fluorescence images were obtained every 30 min. In contrast to rapid leakage of DAF-2 T and DAF-4 T, DCI-DA Cal-T was well-retained in HeLa cells. Additionally, to evaluate the intracellular retention of fluorescence probes themselves, we performed long-term postincubation after loading fluorescence probes (Figure 4j–l). HeLa cells loaded with DCI-DA Cal-AM, DAF-2 DA, or DAF-4 DA were postincubated for 3 h, and the fluorescence increment on addition of NOC 7 was measured. In the case of DAF-2 DA and DAF-4 DA, there was no change of the fluorescence images. On the other hand, DCI-DA Cal could apparently monitor the generation of NO. These results suggested that DCI-DA Cal and DCI-DA Cal T have excellent intracellular retention.

Finally, we applied DCI-DA Cal-AM to cultured bovine aortic endothelial cells (BAEC), which are known to produce NO when stimulated with bradykinin. As mentioned above, because DAF-2 and DAF-4 have similar characteristics, we used DAF-2 DA as a control (DAF-2 is the most widely used general-purpose fluorescence probe for NO). The cells were incubated with 10  $\mu\text{M}$  DCI-DA Cal-AM or DAF-2 DA for 60 min at 37  $^\circ\text{C}$  to load fluorescence probes. The fluorescence images were captured before and after stimulation with 0.1  $\mu\text{M}$  bradykinin. As shown in Figure 5a–c, strong green

Scheme 6. Synthetic Scheme for DCI-DA Cal-AM



fluorescence was observed only when DCI-DA Cal-AM was used, while DAF-2 DA could not monitor well the NO generation. To confirm that this increase of fluorescence

intensity was derived from the reaction product of DCI-DA Cal with NO, we used an inhibitor of NO synthesis, L-NAME (Figure 5c,d). Pretreatment with L-NAME abrogated the

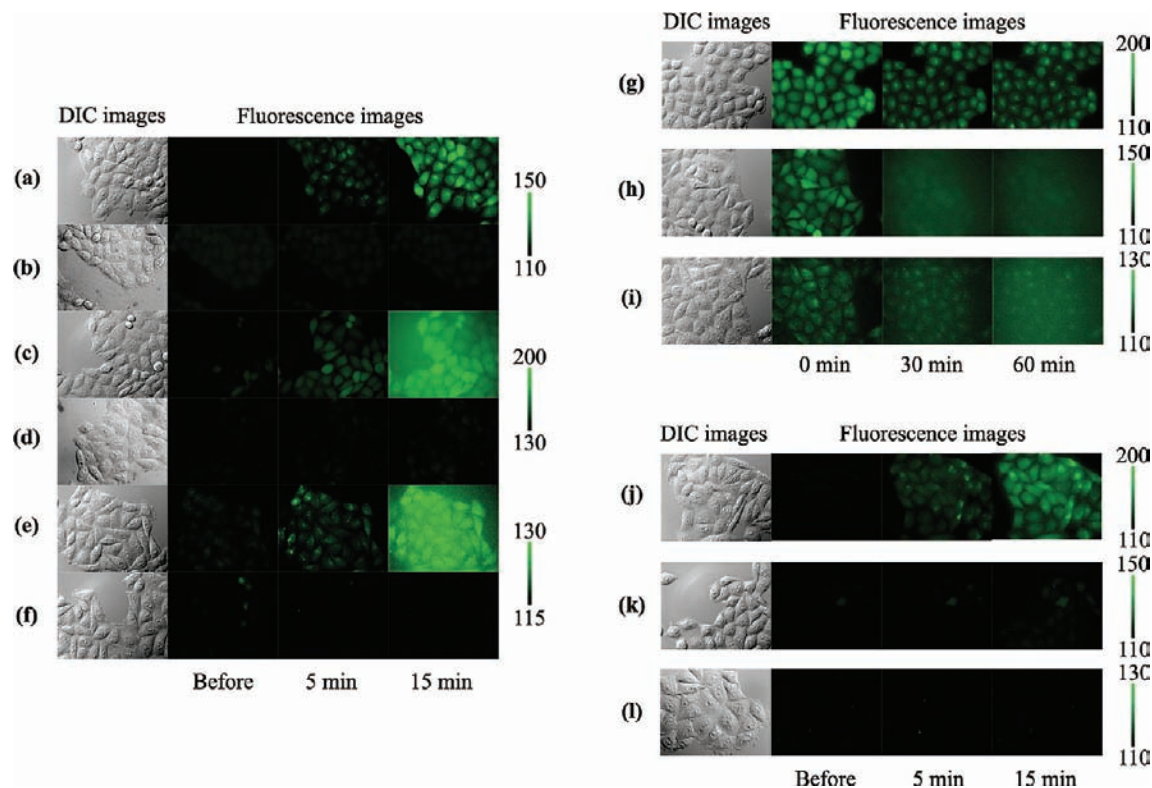


**Figure 4.** NO detection by DCI-DA Cal-AM, DAF-2 DA, and DAF-4 DA in living cells. Fluorescence and DIC images of HeLa cells loaded with  $10 \mu\text{M}$  (0.1% DMSO as a cosolvent) DCI-DA Cal-AM (a, b, g, j), DAF-2 DA (c, d, h, k), or DAF-4 DA (e, f, i, l) for 30 min are shown. (a, c, e) The change of fluorescence images after addition of NOC 7 (final  $100 \mu\text{M}$ ) was measured at 5 and 15 min. (b, d, f) The change of fluorescence intensity without addition of NOC 7 is shown. (g–i) The leakage of DCI-DA Cal T, DAF-2 T, and DAF-4 T. NOC 7 (final  $100 \mu\text{M}$ ) was added for 10 min and then washed out twice. The fluorescence images were observed for 60 min. (j–l) Intracellular retention of fluorescence probes. After loading the fluorescence probes, HeLa cells were postincubated for 3 h and then NOC 7 (final  $100 \mu\text{M}$ ) was added, and fluorescence images were observed for 15 min.



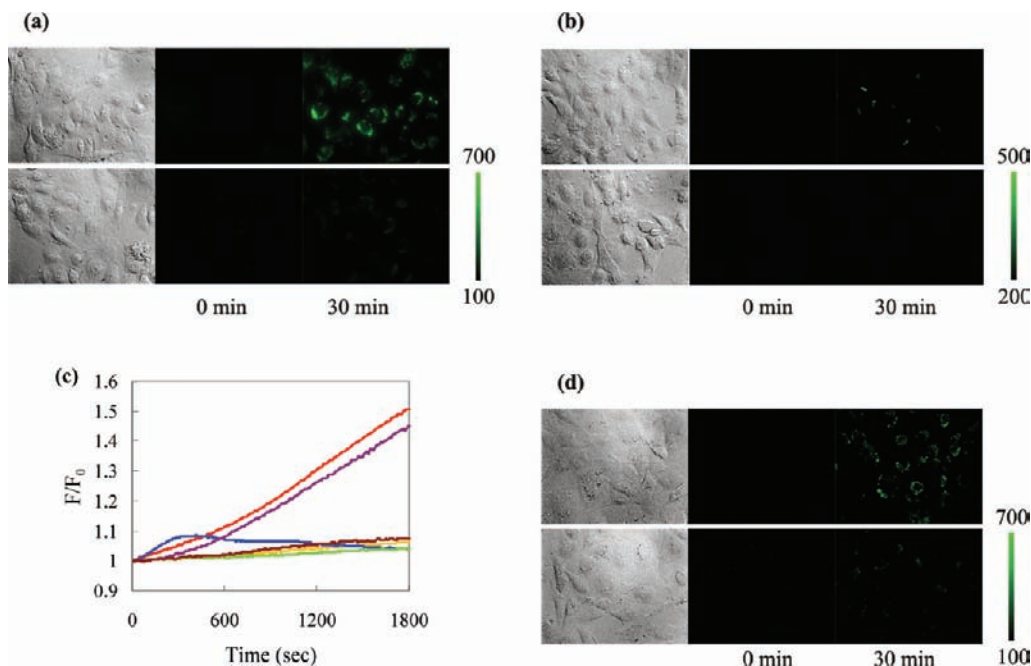


**Figure 5.** Detection of NO produced by BAEC: (a, b, d) fluorescence images and DIC images of BAEC stained with 10  $\mu\text{M}$  DCI-DA Cal-AM (a, d) or DAF-2 DA (b) for 60 min. After loading, DCI-DA Cal-AM and DAF-2 DA were washed out twice, and postincubation was carried out for 30 min. (a, b) Fluorescence images were measured with (upper) or without (lower) 0.1  $\mu\text{M}$  bradykinin stimulation for 30 min. (c) Ratio of the average fluorescence intensity of BAEC ( $n \geq 10$ ) loaded with 10  $\mu\text{M}$  DCI-DA Cal-AM (red, orange, purple, brown) or DAF-2 DA (blue, green), with (red, blue, purple, brown) or without (orange, green) 0.1  $\mu\text{M}$  bradykinin stimulation. One millimolar D-NAME (purple) or L-NAME (brown) was also added. (d) Fluorescence images of BAEC with 1 mM D-NAME (upper) or L-NAME (lower). Exposure time was 200 ms, and ND was 12%.

fluorescence increment.<sup>38</sup> On the other hand, when BAEC were pretreated with D-NAME, the fluorescence increase was unaffected because D-arginine has little influence on NO synthesis. These results indicated that, in a system providing slow release of NO,<sup>39</sup> visualization of low levels of NO depends critically on the lack of leakage of the fluorescence probes and the fluorescence product from the cells.

## Conclusion

In order to develop fluorescence probes that offer high sensitivity inside living cells, efficient retention of the probes and products within the cells is critical. We found that the IAG of calcein is very effective in improving intracellular retention. We exploited this finding to design and synthesize highly sensitive fluorescence probes, APC and DCI-DA Cal, for hROS or RNS, respectively. We demonstrated that these fluorescence probes and their fluorescent products show good intracellular retention compared with conventional fluorescence probes and are suitable for the visualization of low levels of physiological molecules and for long-term observation in living cells. This design concept is expected to be applicable to a broad range of fluorescence probes and should be especially valuable for developing superior cellular imaging probes based on fluorescein and other cytosol-diffusible fluorophores.

## Experimental Section

**Materials.** General chemicals were of the best grade available, supplied by Tokyo Chemical Industries, Wako Pure Chemical, Aldrich Chemical Co., Dojindo, Acros Organics, and Lancaster Synthesis, and they were used without further purification. DMF was of fluorometric grade (Dojindo). All solvents were used after appropriate distillation or purification.

**Instruments.**  $^1\text{H}$  NMR and  $^{13}\text{C}$  NMR spectra were recorded on a JEOL JNM-LA300 instrument (300 MHz for  $^1\text{H}$  NMR and 75

MHz for  $^{13}\text{C}$  NMR) or a JEOL JNM-LA400 instrument (400 MHz for  $^1\text{H}$  NMR and 100 MHz for  $^{13}\text{C}$  NMR);  $\delta$  values are in ppm relative to tetramethylsilane. Mass spectra (MS) were measured with a JEOL JMS-T100LC AccuToF for ESI. UV–visible spectra were obtained on a Shimadzu UV-1650. Fluorescence spectroscopic studies were performed on a Hitachi F4500.

**Fluorometric Analysis.** The slit width was 2.5 nm for both excitation and emission. The photon multiplier voltage was 300 V. Relative fluorescence quantum efficiencies of calcein, **2**, APC, DCI-DA Cal, and DCI-DA Cal T were obtained by comparing the area under the emission spectrum of the test sample excited at 490 nm with that of a solution of fluorescein in 0.1 M sodium phosphate buffer at pH 7.4, which has a quantum efficiency of 0.85.

**HPLC Analysis.** HPLC analysis was performed on an Inertsil ODS-3 (4.6  $\times$  250 mm) column (GL Sciences Inc.) using an HPLC system composed of a pump (PU-980, JASCO) and a detector (MD-2015 or FP-2025, JASCO).

**HPLC Preparation.** Preparative HPLC were performed on an Inertsil ODS-3 (10.0  $\times$  250 mm) column (GL Sciences Inc.) using an HPLC system composed of a pump (PU-2080, JASCO) and a detector (MD-2010, JASCO).

**Fluorescence Microscopy.** Fluorescence images were captured using an Olympus IX 71 with a cooled CCF camera (Coolsnap HQ, Olympus), a xenon lamp (AH2RX-T, Olympus) with a BP-470–490 excitation filter, and a BA-510–550 emission filter, or with a BP-490–500 excitation filter and BA-515–560 emission filter.

**Methods of Experiments Using Living Cells.** HeLa cells were cultured in Dulbecco's modified Eagle's medium (DMEM) supplemented with 10% (v/v) fetal bovine serum, penicillin (100 units/mL), and streptomycin (100  $\mu\text{g}/\text{mL}$ ) in a humidified incubator containing 5%  $\text{CO}_2$  gas. For fluorescence microscopy, HeLa cells were plated in a 35-mm glass-bottomed dish (MatTek Corp.) and cultured overnight in DMEM. HL-60 cells were cultured in Roswell Park Memorial Institute (RPMI) medium supplemented with 10% (v/v) fetal bovine serum, penicillin (100 units/mL), and streptomycin

(100  $\mu\text{g/mL}$ ) in a humidified incubator containing 5%  $\text{CO}_2$  in air. For fluorescence microscopy, HL-60 cells were plated in a 35-mm glass-bottomed dish (MatTek Corporation) in RPMI. BAEC cells were cultured in Dulbecco's modified Eagle's medium (DMEM) supplemented with 10% (v/v) fetal bovine serum, penicillin (100 units/mL), streptomycin (100  $\mu\text{g/mL}$ ), and amphotericin B (0.25  $\mu\text{g/mL}$ ) in a humidified incubator containing 5%  $\text{CO}_2$  gas. For fluorescence microscopy, BAEC cells were plated in a 35-mm glass-bottomed dish (MatTek Corp.) and cultured overnight in DMEM.

**FCM.** We used a BD LSR II flow cytometer (BD Biosciences), with FlowJo (Digital Biology). The excitation wavelength was 488 nm, and the emission was detected via a FITC filter ( $530 \pm 30$  nm).

**Method of Determination of the Concentration of Generated Superoxide in X/XO System.** Xanthine (10  $\mu\text{M}$ ) was added to cytochrome *c* (10  $\mu\text{M}$ ) and xanthine oxidase (1.73 mU/mL), and the absorbance at 550 nm was measured. The concentration of generated superoxide was calculated from the increase of absorbance, with  $\epsilon_{550} = 21.6 \text{ mM}^{-1} \text{ cm}^{-1}$ .

**Cyclic Voltammetry.** Cyclic voltammetry was performed on a 630B electrochemical analyzer (ALS). A three-electrode arrangement in a single cell was used for the measurements: a Pt wire as the auxiliary electrode, a glass carbon electrode as the working electrode, and an Ag/Ag<sup>+</sup> electrode as the reference electrode. The sample solutions contained a 1.0 mM sample in 0.1 M sodium phosphate buffer (pH 4 and 8), and argon was bubbled for 10 min before each measurement. Obtained potentials (vs Ag/Ag<sup>+</sup>) were converted to those vs SCE by subtracting 0.030 V.

**6'-Hydroxy-4'-[N,N'-bis(carboxymethyl)aminomethyl]-3'-oxo-fluorescein Diethyl Ester (1).** A suspension of fluorescein (0.500 g, 1.50 mmol), diethyl iminodiacetate (2.85 mg, 15.1 mmol), and paraformaldehyde (0.450 g, 15.0 mmol) in 35 mL of  $\text{CH}_3\text{CN}$  and 15 mL of  $\text{H}_2\text{O}$  was refluxed for 20 h. After the solution had cooled to room temperature, the solvent was removed by evaporation. Purification of the residue by HPLC provided pure **1** as a yellow powder (192 mg, 0.360 mmol, 24% yield). <sup>1</sup>H NMR (300 MHz,  $\text{CD}_3\text{OD}$ )  $\delta$ : 1.28 (t, 6H,  $J = 7.1$  Hz), 4.18 (s, 4H), 4.29 (q, 4H,  $J = 7.1$  Hz), 4.78 (s, 2H), 6.59 (dd, 1H,  $J = 8.8$  Hz, 2.01 Hz), 6.62 (d, 1H,  $J = 8.8$  Hz), 6.66 (d, 1H,  $J = 8.8$  Hz), 6.75 (d, 1H,  $J = 8.8$  Hz), 6.89 (d, 1H,  $J = 2.0$  Hz), 7.22 (d, 1H,  $J = 7.3$  Hz), 7.69–7.80 (m, 2H), 8.02 (d, 1H,  $J = 7.7$  Hz). <sup>13</sup>C NMR (100 MHz,  $\text{CD}_3\text{OD}$ )  $\delta$ : 14.3, 55.1, 63.5, 103.9, 105.4, 111.4, 112.3, 113.4, 114.2, 116.3, 119.2, 125.5, 126.2, 128.2, 130.2, 131.3, 132.2, 136.6, 153.2, 153.5, 161.5, 161.8, 162.2, 168.6, 171.2. HRMS (ESI<sup>+</sup>):  $m/z$  calculated for  $[\text{M} + \text{Na}]^+$  556.1584, found 556.1600.

**6'-Hydroxy-4'-[N,N'-bis(carboxymethyl)aminomethyl]-3'-oxo-fluorescein (2).** A solution of **1** (68.7 mg, 0.129 mmol) and KOH (0.570 g, 0.0100 mmol) in 10 mL of MeOH was stirred at room temperature for 3 h and then acidified with aqueous HCl. The solvent was removed by rotary evaporation and the residue was subjected to HPLC to provide pure **2** as a yellow powder (59.2 mg, 0.124 mmol, 92% yield). <sup>1</sup>H NMR (400 MHz,  $\text{CD}_3\text{OD}$ )  $\delta$ : 4.08 (s, 4H), 4.77 (s, 2H), 6.47–6.52 (m, 2H), 6.58 (d, 1H,  $J = 8.8$  Hz), 6.66 (d, 1H,  $J = 8.8$  Hz), 6.85 (d, 1H,  $J = 0.8$  Hz), 7.13 (d, 1H,  $J = 8.0$  Hz), 7.59–7.69 (m, 2H), 7.92 (d, 1H,  $J = 7.2$  Hz). <sup>13</sup>C NMR (100 MHz,  $\text{CD}_3\text{OD}$ )  $\delta$ : 49.8, 55.2, 104.2, 104.3, 111.3, 112.3, 113.3, 114.2, 125.5, 126.1, 128.1, 130.0, 131.3, 132.6, 136.6, 153.3, 153.4, 153.6, 161.2, 161.6, 169.1, 171.2. HRMS (ESI<sup>-</sup>):  $m/z$  calculated for  $[\text{M} - \text{H}]^-$  476.0982, found 476.0979.

**3',6'-Bis(acetyloxy)-4'-[N,N'-bis(carboxymethyl)aminomethyl]fluorescein diacetyloxymethyl ester (2-AM).** A solution of **2** (37.1 mg, 0.0777 mmol), 1.5 mL of  $\text{Ac}_2\text{O}$ , and 1 mL of pyridine was stirred under argon at room temperature for 3 h. The solvent was removed by rotary evaporation. The residue was stirred with *N*-ethyl-diisopropylamine (402 mg, 3.10 mmol) and bromomethyl acetate (476 mg, 3.11 mmol) in 5 mL of DMF under argon at room temperature overnight. The resulting mixture was acidified with acetic acid and extracted with AcOEt. The organic layer was dried over anhydrous sodium sulfate and the solvent was removed by

rotary evaporation. The residue was subjected to HPLC to provide pure **2-AM** as a yellow powder (11.7 mg, 0.0166 mmol, 22% yield). <sup>1</sup>H NMR (400 MHz,  $\text{DMSO}-d_6$ )  $\delta$ : 1.95 (s, 6H), 2.22 (s, 3H), 2.24 (s, 3H), 3.62 (s, 4H), 4.05 (s, 2H), 5.58 (s, 4H), 6.73 (d, 1H,  $J = 8.8$  Hz), 6.83 (d, 1H,  $J = 8.0$  Hz), 6.88 (d, 1H,  $J = 8.8$  Hz), 6.89 (dd, 1H,  $J = 8.0$  Hz, 2.0 Hz), 7.22 (d, 1H,  $J = 2.0$  Hz), 7.31 (d, 1H,  $J = 7.6$  Hz), 7.68–7.78 (m, 2H), 8.00 (d, 1H,  $J = 7.6$  Hz). <sup>13</sup>C NMR (100 MHz,  $\text{DMSO}-d_6$ )  $\delta$ : 20.4, 20.5, 20.8, 45.2, 53.6, 78.7, 81.2, 110.6, 116.0, 116.1, 118.2, 118.7, 119.1, 124.0, 125.1, 125.3, 127.9, 128.9, 130.6, 136.0, 149.9, 150.6, 151.2, 152.0, 152.3, 168.4, 168.9, 169.0, 169.3, 169.7. HRMS (ESI<sup>+</sup>):  $m/z$  calculated for  $[\text{M} + \text{Na}]^+$  728.1591, found 728.1607.

**6'-Hydroxy-4',5'-bis[N,N'-bis(carboxymethyl)aminomethyl]-3'-oxo-fluorescein Tetraethyl Ester (3).** A suspension of fluorescein (1.01 g, 3.04 mmol), diethyl iminodiacetate (1.6 mg, 8.46 mmol), and paraformaldehyde (0.310 g, 10.3 mmol) in 35 mL of  $\text{CH}_3\text{CN}$  and 15 mL of  $\text{H}_2\text{O}$  was refluxed for 2 days. After the solution had cooled to room temperature, the solvent was removed by evaporation. Purification of the residue by silica gel column chromatography with  $\text{CH}_2\text{Cl}_2$  provided pure **3** as a yellow powder (2.08 g, 2.83 mmol, 93% yield). <sup>1</sup>H NMR (300 MHz,  $\text{CD}_3\text{CN}$ )  $\delta$ : 1.20 (t, 12H,  $J = 7.3$  Hz), 3.56 (s, 8H), 4.14 (q, 8H,  $J = 7.3$  Hz), 4.25 (s, 2H), 4.26 (s, 2H), 6.50 (d, 2H,  $J = 8.8$  Hz), 6.58 (d, 2H,  $J = 8.8$  Hz), 7.16 (d, 1H,  $J = 7.3$  Hz), 7.64–7.76 (m, 2H), 7.95 (d, 1H,  $J = 8.1$  Hz). <sup>13</sup>C NMR (100 MHz,  $\text{CD}_3\text{OD}$ )  $\delta$ : 14.4, 49.9, 55.6, 63.0, 107.6, 112.0, 113.9, 125.5, 126.3, 128.1, 131.2, 131.4, 136.6, 152.3, 161.5, 161.9, 170.2, 171.0. HRMS (ESI<sup>+</sup>):  $m/z$  calculated for  $[\text{M} + \text{H}]^+$  735.2762, found 735.2752.

**4',5'-Bis[N,N'-bis(carboxymethyl)aminomethyl]-3'-oxo-6'-(4''-nitro)phenoxyfluorescein Tetraethyl Ester (4).** **3** (1.35 g, 1.84 mmol) was stirred with 4-fluoronitrobenzene (0.290 g, 2.06 mmol) and  $\text{Na}_2\text{CO}_3$  (0.580 g, 5.47 mmol) in 5 mL of DMSO at 90 °C for 3 h. After the solution had cooled to room temperature, the resulting mixture was acidified with aqueous HCl and extracted with  $\text{CH}_2\text{Cl}_2$ . The organic layer was dried over anhydrous sodium sulfate and evaporated in vacuo. The residue was purified by silica gel column chromatography with 2:1 *n*-hexane/ $\text{CH}_2\text{Cl}_2$  to give to **4** (252 mg, 0.294 mmol, 16% yield). <sup>1</sup>H NMR (300 MHz,  $\text{CD}_3\text{CN}$ )  $\delta$ : 1.09 (t, 6H,  $J = 7.3$  Hz), 1.19 (t, 6H,  $J = 7.3$  Hz), 3.60 (s, 4H), 3.69 (s, 4H), 3.96 (q, 4H,  $J = 7.3$  Hz), 4.12 (q, 4H,  $J = 7.3$  Hz), 4.23 (s, 2H), 4.31 (d, 1H,  $J = 14.6$  Hz), 4.44 (d, 1H,  $J = 14.6$  Hz), 6.56 (d, 1H,  $J = 8.8$  Hz), 6.63 (d, 1H,  $J = 8.8$  Hz), 6.70 (d, 1H,  $J = 8.8$  Hz), 6.79 (d, 1H,  $J = 8.8$  Hz), 7.07 (d, 2H,  $J = 8.8$  Hz), 7.22 (d, 1H,  $J = 7.3$  Hz), 7.64–7.78 (m, 2H), 7.97 (d, 1H,  $J = 7.4$  Hz), 8.17 (d, 2H,  $J = 8.8$  Hz). <sup>13</sup>C NMR (75 MHz,  $\text{CD}_3\text{CN}$ )  $\delta$ : 14.5, 47.4, 49.5, 54.9, 55.3, 61.1, 61.8, 83.7, 109.8, 110.5, 114.1, 116.6, 117.3, 118.3, 118.7, 119.8, 124.8, 125.8, 126.9, 127.4, 129.0, 129.7, 131.1, 136.4, 144.1, 150.6, 152.2, 153.6, 156.2, 161.1, 163.3, 169.8, 171.8, 171.9. HRMS (ESI<sup>-</sup>):  $m/z$  calculated for  $[\text{M} - \text{H}]^-$  854.2772, found 854.2802.

**4',5'-Bis[N,N'-bis(carboxymethyl)aminomethyl]-3'-oxo-6'-(4''-amino)phenoxyfluorescein Tetraethyl Ester (5).** To a solution of 363 mg (0.424 mmol) of **4** in a mixture of 1 mL of MeOH and 9 mL of  $\text{CH}_2\text{Cl}_2$  was added Pd/C (10%). The resulting mixture was stirred under  $\text{H}_2$  at room temperature for 1 h. Palladium/carbon was removed by filtration and the filtrate was evaporated in vacuo. The residue was purified by silica gel column chromatography with 99:1  $\text{CH}_2\text{Cl}_2/\text{MeOH}$ , followed by HPLC to provide pure **5** as a yellow powder (253 mg, 0.306 mmol, 72% yield). <sup>1</sup>H NMR (400 MHz,  $\text{CD}_3\text{CN}$ )  $\delta$ : 1.06 (t, 6H,  $J = 7.3$  Hz), 1.18 (t, 6H,  $J = 7.3$  Hz), 3.58 (s, 4H), 3.74 (s, 4H), 3.93 (q, 4H,  $J = 7.3$  Hz), 4.14 (q, 4H,  $J = 7.3$ ), 4.30 (d, 1H,  $J = 14.1$  Hz), 4.32 (s, 2H), 4.41 (d, 1H,  $J = 14.1$  Hz), 6.32 (d, 1H,  $J = 8.8$  Hz), 6.51 (d, 1H,  $J = 8.8$  Hz), 6.55 (d, 1H,  $J = 8.8$  Hz), 6.57 (d, 1H,  $J = 8.8$  Hz), 6.59 (d, 2H,  $J = 8.8$  Hz), 6.74 (d, 2H,  $J = 8.8$  Hz), 7.15 (d, 1H,  $J = 7.3$  Hz), 7.60–7.72 (m, 2H), 7.91 (d, 1H,  $J = 7.3$  Hz). <sup>13</sup>C NMR (100 MHz,  $\text{CD}_3\text{CN}$ )  $\delta$ : 14.5, 46.9, 49.6, 55.0, 55.3, 61.0, 61.9, 84.3, 109.8, 110.8, 112.2,

113.8, 113.9, 116.0, 116.3, 118.3, 122.1, 124.9, 125.7, 127.6, 128.9, 129.0, 130.9, 136.3, 146.1, 147.4, 150.9, 152.0, 153.7, 160.4, 161.0, 169.9, 171.9, 172.2. HRMS (ESI<sup>-</sup>): *m/z* calculated for [M - H]<sup>-</sup> 824.3031, found 824.3073.

**4',5'-Bis[*N,N'*-bis(carboxymethyl)aminomethyl]-3'-oxo-6'-(4''-amino)phenoxyfluorescein (APC).** A solution of **5** (42.2 mg, 0.0511 mmol) and KOH (2.28 g, 40.0 mmol) in 40 mL of MeOH was stirred at room temperature for 12 h and then acidified with aqueous HCl. The solvent was removed by rotary evaporation and the residue was subjected to HPLC to provide pure APC as a yellow powder (24.5 mg, 0.0343 mmol, 67% yield). <sup>1</sup>H NMR (400 MHz, CD<sub>3</sub>OD) δ: 4.15 (s, 4H), 4.19 (s, 4H), 4.93 (s, 2H), 5.00 (s, 2H), 6.62 (d, 1H, *J* = 9.3 Hz), 6.75 (d, 1H, *J* = 8.8 Hz), 6.79 (d, 1H, *J* = 8.8 Hz), 6.88 (d, 1H, *J* = 9.3 Hz), 7.26 (d, 2H, *J* = 8.3 Hz), 7.30 (d, 1H, *J* = 7.8 Hz), 7.37 (d, 2H, *J* = 8.3 Hz), 7.69–7.80 (m, 2H), 8.00 (d, 1H, *J* = 7.3 Hz). <sup>13</sup>C NMR (100 MHz, DMSO-*d*<sub>6</sub>) δ: 46.3, 47.4, 53.8, 54.1, 82.6, 109.3, 112.8, 113.0, 113.9, 115.2, 118.1, 120.3, 122.1, 124.1, 124.9, 125.7, 128.6, 128.9, 130.3, 135.8, 149.9, 150.8, 152.5, 157.4, 158.2, 158.5, 159.3, 168.7, 171.6, 171.7. HRMS (ESI<sup>+</sup>): *m/z* calculated for [M + H]<sup>+</sup> 714.1935, found 714.1943.

**4',5'-Bis[*N,N'*-bis(carboxymethyl)aminomethyl]-6'-(4''-amino)phenoxyfluorescein Tetraacetoxymethyl Ester (APC-AM).** A solution of APC (23.1 mg, 0.0324 mmol), *N*-ethyl-diisopropylamine (168 mg, 1.30 mmol), and bromomethyl acetate (199 mg, 1.30 mmol) in 5 mL of DMF was stirred under argon at room temperature overnight. The resulting mixture was acidified with acetic acid and extracted with AcOEt. The organic layer was dried over anhydrous sodium sulfate and the solvent was removed by rotary evaporation. The residue was subjected to HPLC to provide pure APC-AM as a yellow powder (6.8 mg, 0.00679 mmol, 21% yield). <sup>1</sup>H NMR (300 MHz, CDCl<sub>3</sub>) δ: 2.01 (s, 6H), 2.08 (s, 6H), 3.72 (s, 2H), 3.74 (s, 2H), 3.88 (s, 4H), 4.28 (d, 1H, *J* = 14.1 Hz), 4.32 (d, 1H, *J* = 12.6), 4.42 (d, 1H, *J* = 12.6 Hz), 4.62 (d, 1H, *J* = 14.1 Hz), 5.65 (s, 4H), 5.81 (s, 2H), 5.81 (s, 2H), 6.36 (d, 1H, *J* = 9.0), 6.56 (d, 1H, *J* = 9.0 Hz), 6.59 (d, 1H, *J* = 8.8 Hz), 6.62 (d, 1H, *J* = 8.8 Hz), 6.65 (d, 2H, *J* = 8.6 Hz), 6.80 (d, 2H, *J* = 8.2 Hz), 7.24 (d, 1H, *J* = 7.7 Hz), 7.59–7.71 (m, 2H), 8.49 (d, 1H, *J* = 7.3 Hz). <sup>13</sup>C NMR (100 MHz, CDCl<sub>3</sub>) δ: 20.6, 46.3, 48.7, 53.6, 53.8, 77.2, 79.1, 79.5, 83.6, 108.0, 110.0, 111.4, 113.2, 113.4, 114.4, 116.2, 121.4, 124.1, 125.1, 127.0, 128.2, 128.5, 129.8, 135.0, 143.4, 147.3, 150.1, 151.2, 152.6, 159.4, 159.9, 169.2, 169.5, 169.6, 170.1. HRMS (ESI<sup>-</sup>): *m/z* calculated for [M - H]<sup>-</sup> 1000.2624, found 1000.2636.

**3-Amino-2',7'-dichloro-6'-hydroxy-4',5'-bis[*N,N'*-bis(carboxymethyl)aminomethyl]-3'-oxo-4-nitrofluorescein Tetraethyl Ester (7).** A suspension of **6** (100 mg, 0.217 mmol), diethyl iminodiacetate (130 mg, 0.687 mmol), and paraformaldehyde (56.6 mg, 1.88 mmol) in 3.5 mL of CH<sub>3</sub>CN and 1.5 mL of H<sub>2</sub>O was refluxed for 2 days. After the solution had cooled to room temperature, the solvent was removed by evaporation. Purification of the residue by column chromatography (silica gel, CH<sub>2</sub>Cl<sub>2</sub>/AcOEt, stepwise) provided pure **7** as a yellow powder (166 mg, 0.192 mmol, 88% yield). <sup>1</sup>H NMR (300 MHz, CD<sub>3</sub>CN) δ: 1.28 (t, 12H, *J* = 7.1 Hz), 3.60 (s, 8H), 4.21 (q, 8H, *J* = 7.3 Hz), 4.25 (d, 2H, *J* = 14.5 Hz), 4.44 (d, 2H, *J* = 14.5 Hz), 6.38 (d, 1H, *J* = 8.6 Hz), 6.78 (s, 2H), 8.46 (d, 1H, *J* = 8.6 Hz). <sup>13</sup>C NMR (100 MHz, CDCl<sub>3</sub>) δ: 14.1, 48.8, 54.1, 61.3, 82.4, 108.8, 109.9, 109.9, 112.3, 117.9, 127.6, 132.2, 134.7, 143.5, 148.1, 156.1, 159.4, 168.5, 170.3. HRMS (ESI<sup>+</sup>): *m/z* calculated for [M + Na]<sup>+</sup> 885.1765, found 885.1770.

**3,4-Diamino-2',7'-dichloro-6'-hydroxy-4',5'-bis[*N,N'*-bis(carboxymethyl)aminomethyl]-3'-oxo-fluorescein Tetraethyl Ester (8).** To a solution of 166 mg (0.192 mmol) of **7** in a mixture of 1 mL of MeOH and 9 mL of CH<sub>2</sub>Cl<sub>2</sub> was added palladium/carbon (10%). The resulting mixture was stirred under H<sub>2</sub> at room temperature for 1 h. Pd/C was removed by filtration and the filtrate was evaporated in vacuo. The residue was purified by silica gel column chromatography with CH<sub>2</sub>Cl<sub>2</sub>/AcOEt, followed by HPLC to provide pure **8** as a yellow powder (97.0 mg, 0.116 mmol,

60% yield). <sup>1</sup>H NMR (300 MHz, CDCl<sub>3</sub>) δ: 1.27 (t, 12 H, *J* = 7.3 Hz), 3.61 (s, 8H), 4.21 (q, 8H, *J* = 7.3 Hz), 4.23 (d, 2H, *J* = 14.6 Hz), 4.43 (d, 2H, *J* = 14.6 Hz), 6.33 (d, 1H, *J* = 8.0 Hz), 6.82 (s, 2H), 6.97 (d, 1H, *J* = 8.0 Hz). <sup>13</sup>C NMR (100 MHz, CDCl<sub>3</sub>) δ: 14.0, 48.8, 54.0, 61.1, 82.3, 109.3, 110.6, 111.8, 112.3, 117.1, 123.0, 128.1, 134.1, 135.8, 142.1, 148.3, 155.2, 170.1, 170.3. HRMS (ESI<sup>+</sup>): *m/z* calculated for [M + H]<sup>+</sup> 833.2204, found 833.2235.

**3,4-Diamino-2',7'-dichloro-6'-hydroxy-4',5'-bis[*N,N'*-bis(carboxymethyl)aminomethyl]-3'-oxo-fluorescein (DCI-DA Cal).** A solution of 97.0 mg (0.116 mmol) of **8** and KOH (2.85 g, 0.0500 mmol) in 50 mL of MeOH was stirred at room temperature for 2.5 h, and then acidified with aqueous HCl. The solvent was removed by rotary evaporation and the residue was subjected to HPLC to provide pure DCI-DA Cal as a yellow powder (80.0 mg, 0.111 mmol, 96%). <sup>1</sup>H NMR (300 MHz, CD<sub>3</sub>OD) δ: 3.78 (s, 8H), 4.52 (s, 4H), 6.23 (d, 1H, *J* = 7.3 Hz), 6.73 (s, 2H), 7.09 (d, 1H, *J* = 7.3 Hz). <sup>13</sup>C NMR (100 MHz, CD<sub>3</sub>OD) δ: 55.3, 83.0, 110.4, 110.5, 112.2, 113.4, 116.2, 118.5, 119.1, 129.9, 150.3, 156.4, 161.8, 162.1, 171.6, 172.3. HRMS (ESI<sup>+</sup>): *m/z* calculated for [M + H]<sup>+</sup> 721.0952, found 721.0993.

**9-(4'-Carboxybenzotriazol-5'-yl)-2,7-dichloro-6-hydroxy-4,5-bis[*N,N'*-bis(carboxymethyl)aminomethyl][3H]xanthen-3-one (DCI-DA Cal-T).** A solution of DCI-DA Cal (10.0 mg, 0.0139 mmol) in 3 mL of MeOH was bubbled with NO gas. The solvent was removed by rotary evaporation and the residue was subjected to HPLC to provide pure DCI-DA Cal-T as a yellow powder (7.2 mg, 0.00983 mmol, 70% yield). <sup>1</sup>H NMR (300 MHz, CD<sub>3</sub>OD) δ: 3.76 (s, 8H), 4.53 (s, 4H), 6.78 (s, 2H), 7.19 (d, 1H, *J* = 8.8 Hz), 8.31 (d, 1H, *J* = 8.8 Hz). HRMS (ESI<sup>+</sup>): *m/z* calculated for [M + H]<sup>+</sup> 730.0591, found 730.0573.

**3-Amino-2',7'-dichloro-6'-hydroxy-4',5'-bis[*N,N'*-bis(carboxymethyl)aminomethyl]-3'-oxo-4-nitrofluorescein (9).** A solution of **7** (164 mg, 0.190 mmol) and KOH (2.85 g, 50.0 mmol) in 50 mL of MeOH was stirred at room temperature for 4 h and then acidified with aqueous HCl. The solvent was removed by rotary evaporation and the residue was subjected to HPLC to provide pure **9** as a yellow powder (131 mg, 0.175 mmol, 92% yield). <sup>1</sup>H NMR (300 MHz, CD<sub>3</sub>OD) δ: 3.83 (s, 8H), 4.57 (s, 4H), 6.42 (d, 1H, *J* = 8.8 Hz), 6.94 (s, 2H) 8.47 (d, 1H, *J* = 8.8 Hz). <sup>13</sup>C NMR (100 MHz, CD<sub>3</sub>OD) δ: 49.8, 55.3, 82.5, 110.5, 110.8, 111.1, 112.9, 118.7, 129.5, 133.4, 136.0, 144.9, 150.0, 156.7, 161.3, 170.1, 172.5. HRMS (ESI<sup>+</sup>): *m/z* calculated for [M + H]<sup>+</sup> 751.0694, found 751.0669.

**3-Amino-2',7'-dichloro-3',6'-bis(acetoxymethoxy)-4',5'-bis[*N,N'*-bis(carboxymethyl)aminomethyl]-4-nitrofluorescein Tetraacetoxymethyl Ester (10).** A solution of **9** (51.2 mg, 0.0681 mmol), *N*-ethyl-diisopropylamine (353 mg, 2.73 mmol), and bromomethyl acetate (421 mg, 2.75 mmol) in 8 mL of CH<sub>3</sub>CN was stirred under argon at room temperature overnight. The resulting mixture was acidified with acetic acid and extracted with AcOEt. The organic layer was dried over anhydrous sodium sulfate and the solvent was removed by rotary evaporation. The residue was subjected to HPLC to provide pure **10** as a yellow powder (15.4 mg, 0.0130 mmol, 20% yield). <sup>1</sup>H NMR (300 MHz, CDCl<sub>3</sub>) δ: 2.08 (s, 12H), 2.17 (s, 6H), 3.75 (s, 8H), 4.29 (d, 2H, *J* = 12.5 Hz), 4.40 (d, 2H, *J* = 12.5 Hz), 5.70 (s, 8H), 5.79 (s, 4H), 6.49 (d, 1H, *J* = 8.8 Hz), 6.94 (s, 2H), 8.50 (d, 1H, *J* = 8.8 Hz). HRMS (ESI<sup>+</sup>): *m/z* calculated for [M + Na]<sup>+</sup> 1205.1781, found 1205.1778.

**3,4-Diamino-2',7'-dichloro-3',6'-bis(acetoxymethoxy)-4',5'-bis[*N,N'*-bis(carboxymethyl)aminomethyl]fluorescein Tetraacetoxymethyl Ester (DCI-DA Cal-AM).** To a solution of 15.0 mg (0.0127 mmol) of **10** in a mixture of 3 mL of MeOH and 3 mL of CH<sub>2</sub>Cl<sub>2</sub> was added Pd/C (10%). The resulting mixture was stirred under H<sub>2</sub> at room temperature for 1 h. Palladium/carbon was removed by filtration and the filtrate was evaporated in vacuo. The residue was subjected to HPLC to provide pure DCI-DA Cal-AM as a white powder (4.9 mg, 0.00425 mmol, 33% yield). <sup>1</sup>H NMR (300 MHz, CDCl<sub>3</sub>) δ: 2.08 (s, 12H), 2.16 (s, 6H), 3.75 (s, 8H),

4.26 (d, 2H,  $J = 12.5$  Hz), 4.40 (d, 2H,  $J = 12.5$  Hz), 5.71 (s, 8H), 5.78 (s, 4H), 6.39 (d, 1H,  $J = 8.0$  Hz), 6.96 (s, 2H), 6.99 (d, 1H,  $J = 8.0$  Hz). HRMS (ESI<sup>+</sup>):  $m/z$  calculated for  $[M + Na]^+$  1175.2039, found 1175.2022.

**Acknowledgment.** This study was supported in part by a grant from Hoansha Foundation to T.N. This study was also supported in part by research grants (Grant Nos. 19021010, 19205021, and 20117033 to Y.U.) from the Ministry of Education, Culture, Sports, Science and Technology of the Japanese Government and by a grant from the Kato Memorial Bioscience Foundation to Y.U.

**Supporting Information Available:** pH profiles; fluorescence time course of reactions between APC and hROS; HPLC chromatograms of APC, calcein, DCI-DA Cal, DCI-DA Cal T and reaction mixtures with fluorescence probes and ROS; and assessment of the stability of acetoxymethyl ester protection of DCI-DA Cal-AM. This material is available free of charge via the Internet at <http://pubs.acs.org>.

JA902511P